Pharm Res (2014) 31:2539–2548
DOI 10.1007/s11095-014-1350-2

RESEARCH PAPER

Laurate Permeates the Paracellular Pathway for Small Molecules in the Intestinal Epithelial Cell Model HT-29/B6 via Opening the Tight Junctions by Reversible Relocation of Claudin-5

Isabel Dittmann • Maren Amasheh • Susanne M. Krug • Alexander G. Markov • Michael Fromm • Salah Amasheh

Received: 27 December 2013 / Accepted: 24 February 2014 / Published online: 15 March 2014

ABSTRACT

Purpose To mechanistically analyze effects of the medium-chain fatty acid laurate on transepithelial permeability in confluent monolayers of the intestinal epithelial cell line HT-29/B6, in context with an application as an absorption enhancer improving transepithelial drug permeation.

Methods Transepithelial resistance and apparent permeability for paracellular flux markers was measured using Ussing-type chambers. Two-path impedance spectroscopy was employed to differentiate between transcellular and paracellular resistance, and confocal imaging and Western blotting was performed.

Results Laurate resulted in a substantial and reversible decrease in transepithelial resistance by 50% which was attributed to a decrease in paracellular resistance. Simultaneously, an increase in permeability for fluorescein (330 Da) was detected, while permeabilities for 4 kDa FITC-dextran and sulpho-NHS-SS-biotin (607 Da) remained unaltered. Confocal laser-scanning microscopy revealed a marked reduction of claudin-5, while other tight junction proteins including tricellulin, a protein preventing the paracellular passage of macromolecules, were not affected.

Conclusions Laurate induces an increase in paracellular permeability for molecules up to a molecular mass of 330 Da by retrieval of claudin-5 from tight junctions without affecting tricellular contacts and the paracellular passage of macromolecules. We hereby provide, for the first time, a mechanistical explanation of laurate-induced permeability enhancement on molecular level.

KEY WORDS absorption enhancer · drug uptake · epithelial cell · tight junctions

ABBREVIATIONS

FITC	Fluorescein isothiocyanate
MCFA	Medium-chain fatty acids
NHS	n-hydroxysuccinimide
TER	Transepithelial resistance
TJ	Tight junctions

INTRODUCTION

Oral drug distribution is a convenient and non-invasive application mode in pharmacotherapy. However, it is limited by substance-specific traits and gastrointestinal bioavailability. In the development of oral drugs, a major challenge is to ensure the effective and levelled passage of a compound across the intestinal epithelium. While lipophilic molecules pass the cell membrane across its lipid bilayer, hydrophilic drugs depend on specific uptake mechanisms. Therefore, one approach to improving drug absorption is to select or modify a substance according to the endogenous epithelial absorptive mechanisms, e.g. by targeting specific intestinal membrane transporters (1–3); another is to specifically alter the epithelial barrier in a way that attains effective drug uptake (4,5). Absorption enhancement attempts the selective and reversible regulation of the paracellular pathway, thereby facilitating the temporary passage of macromolecules. Typically, the paracellular pathway is limited by the tight junction, a belt-like network of strands enclosing and interconnecting the cell

I. Dittmann • S. M. Krug • M. Fromm
Institute of Clinical Physiology, Charité, Campus Benjamin Franklin
12200 Berlin, Germany

M. Amasheh
Department of Gastroenterology
Infectiology and Rheumatology, Division of Nutritional Medicine
Charité, Campus Benjamin Franklin
12200 Berlin, Germany

A. G. Markov
Department of General Physiology, St. Petersburg State University
199034 St. Petersburg, Russian Federation

S. Amasheh (✉)
Institute of Veterinary Physiology, Department of Veterinary Medicine
Freie Universität Berlin, Oertzenweg 19b, 14163 Berlin, Germany
e-mail: salah.amasheh@fu-berlin.de

and its neighbours. The tight junction's molecular composition varies, depending on the type of epithelium and segment within the intestine (6). So far, more than 30 barrier-relevant proteins have been identified, constituting the families of claudins -1 to -27 in mammals (7–9) and TAMPs (tight junction-associated marvel proteins) occludin (10), tricellulin (11) and marvel-D3 (12).

A variety of substances have been investigated with regard to their aptitude as absorption enhancers (13,14). Amongst the requirements are selectivity, reversibility and non-toxicity of the effective substance as well as an understanding of the underlying mechanisms induced in epithelial cells.

Several medium-chain fatty acids (MCFA) have been discussed for their *in vitro* and *in vivo* permeability-enhancing properties (15–17). Caprate (C10) has been approved as part of a rectal suppository and both caprate and caprylate (C8) are components of permeability-enhancing formulations already in clinical trials (5). However, there is evidence for detergent effects of higher concentrations of MCFAs both *in vitro* and *in vivo* with increased permeability related to non-specific solubilization of the epithelial cell membranes rather than TJ-specific paracellular effects (15,18). These findings will require further scrutiny of dosage-related effects and cell viability in different epithelial *in vitro* cell models as well as *in vivo*.

Another risk linked with the opening of the paracellular pathway for larger molecules is the possibility of immunoreactive compounds and noxious agents simultaneously crossing the barrier. Therefore, both reversibility of permeation as well as size-selectivity of absorption enhancing effects need to be examined.

Laurate (C12), a medium-chain fatty acid, is a potential candidate for absorption enhancement as it naturally occurs in a variety of foods such as cow's milk and coconut oil (19,20). Its addition to canola oil has been approved by the US Food and Drug Administration (21). Furthermore, human milk contains significant levels of laurate—up to 6.4% of total fat—which demonstrates biocompatibility of the compound (19,20). As yet, the mechanisms by which laurate affects the epithelial barrier are not fully understood. Laurate induced a rapid decrease in transepithelial resistance in Caco-2 cells, and increased permeability for solutes such as fluorescein and [^{14}C]-mannitol (15).

Different signaling pathways have been suggested for long and short term effects of laurate indicating an involvement of phospholipase C (15).

In order to further resolve the distinct effects of laurate on both transepithelial resistance and permeability, we employed two-path impedance spectroscopy to determine paracellular resistance, as well as flux measurements for paracellular markers of different sizes. and finally tight junction proteins were analyzed which represent the structural correlate of epithelial barrier function.

The goal of our study was to test the hypothesis that the mechanisms underlying the more limited effects of laurate on paracellular permeability are strictly separate from the mechanisms induced by caprate which affects tricellulin, a determinant of paracellular macromolecule permeability (14).

Laurate enhances the permeability for the 330 Da marker fluorescein but not for larger molecules as opposed to caprate which opens the paracellular pathway for macromolecules up to 10 kDa (14). While caprate is being tested in clinical trials as a permeability enhancer and may qualify for drugs of a molecular weight up to 10 kDa (18), laurate appears to be less apt as an absorption enhancer, at most qualifying for the specific uptake enhancement of small molecules of about 300 Da in size.

MATERIALS AND METHODS

Cells and Solutions

Confluent monolayers of the human colon cell line HT-29/B6 are a well-established model epithelium (22) and have recently been used in a detailed analysis of the effects of chitosan and caprate as absorption enhancers (13,14). Monolayers were cultured in 25 cm^2 flasks, containing RPMI1640 with stable L-glutamine, 10% fetal calf serum, and 1% penicillin/streptomycin until confluence at 37°C in a humidified 5% CO_2 atmosphere, as reported previously (13).

For electrophysiological analyses, cells were cultured on Millicell PCF filters (Millipore, Schwalbach, Germany), and experiments were performed after 7 days. For experiments, sodium laurate with a molecular mass of 222,3 g/mol (Sigma Aldrich, Taufkirchen, Germany) was added to Ringer's solution containing 113.6 mM NaCl, 2.4 mM Na_2HPO_4, 0.6 mM NaH_2PO_4, 21 mM $NaHCO_3$, 5.4 mM KCl, 1.2 mM $CaCl_2$, 1.2 mM $MgCl_2$, and 10 mM D(+)-glucose. Cell viability was monitored under different experimental conditions by lactate dehydrogenase (LDH) release assay as recently reported in detail (14).

Transepithelial Resistance and Paracellular Flux Marker Measurements

Permeable supports were mounted in custom-designed Ussing chambers, and water-jacketed gas lifts were filled with 5 ml Ringer's solution on each side. The solution was gassed with 95% O_2 and 5% CO_2, and kept at 37°C. Short current pulses (50 μA, 0.3 s) were applied to induce voltage changes (ΔV) for calculation of transepithelial resistance (TER). Data were corrected by values of the empty filter and bath solution. Paracellular marker flux analyses were performed in Ussing chambers under voltage-clamp conditions (0 mV). 0.4 mM of

dialyzed 4 kDa FITC-labeled dextran was added to the apical side, and basolateral samples were collected every 30 min and replaced by fresh perfusion solution. Three flux periods of 30 min were analyzed after application of laurate compared to controls. Dextran fluxes were calculated from the amount of FITC-dextran in the basolateral compartment and measured with a fluorometer at 520 nm (Tecan Infinite M200, Tecan, Switzerland).

Macromolecule passage across the tight junction employing sulfosuccinimidyl-2-(biotinamido)-ethyl-1,30-dithiopropionate (sulfo-NHS-SS-biotin) was performed as described in detail recently (14). Briefly, cells were apically labeled with sulfo-NHS-SS-biotin (606.7 Da). Subsequently, cells were fixed and mouse anti-Zonula Occludens-1 (Invitrogen, Zymed Labs, San Francisco, CA) was employed for immunofluorescent staining of the apicolateral tight junction complexes.

Two-Path Impedance Spectroscopy

A model of the epithelial resistance (R^{epi}) as a parallel circuit consisting of the transcellular resistance (R^{trans}) and the paracellular resistance (R^{para}) provides the basis for two-path impedance spectroscopy, as described in detail (23). In this model, R^{epi} equals TER of the confluent monolayers minus the contribution of the permeable support. Both the apical and the basolateral membranes act as resistors and capacitors in parallel, and R^{trans} is the sum of both membrane resistors. Application of alternating current (35 $\mu A/cm^2$) with a frequency range of 1.3 Hz to 65 kHz, resulted in changes in epithelial voltage which was detected by phase-sensitive amplifiers (PSM 1700 PsimetriQ phase sensitive multimeter; N4L; 1,286 electrochemical interface; Solartron Schlumberger).

Complex impedance values were calculated and plotted in a Nyquist diagram. This plot yields a semicircle when electrical time constants of apical and basolateral membranes are equal, as was correct for the experiments in this study. R^{trans} and R^{para} were determined from experiments in which impedance spectra and fluxes of fluorescein as a paracellular marker were obtained before and after chelating of extracellular Ca^{2+} with EGTA, which opened the paracellular route and increased the fluorescein flux inversely proportional to changes of R^{para}, as reported previously (23).

Immunohistochemistry

Confocal laser-scanning immunofluorescence microscopy was performed as described in detail recently (13). Briefly, confluent cell monolayers were incubated with laurate, fixed with methanol, and immunofluorescent staining was performed with antibodies raised against occludin, tricellulin, and claudins in concentrations according to the manufacturers' recommendations (Invitrogen, Zymed Labs, San Francisco, CA). Alexa Fluor 488 goat anti-mouse and Alexa Fluor 594 goat anti-rabbit were used as secondary antibodies (Molecular Probes, MoBiTec, Göttingen, Germany). Antibodies were diluted in PBS containing 0.5% Triton X-100. DAPI (4′,6-diamidino-2-phenylindole dihydrochloride) was employed for staining of cell nuclei, and FITC-phalloidin to stain F-actin. Images were obtained employing a confocal laser scanning microscope (LSM 510 Meta, Carl Zeiss, Jena, Germany) with excitation wavelengths of 543, 488, and 405 nm.

Western Blotting

Cells were either homogenized in buffer containing 20 mM Tris, 5 mM $MgCl_2$, 1 mM EDTA and 0.3 mM EGTA for preparation of membrane fractions, or in total lysis buffer containing 10 mM Tris, 150 mM NaCl, 0.5% Triton X-100, and 0.1% SDS, and protease inhibitors, respectively (Complete, Boehringer, Mannheim, Germany). Protein contents were quantified employing BCA Protein assay reagent (Pierce, Rockford, IL, USA) and a plate reader (Tecan, Grodig, Austria). SDS buffer (Laemmli) was added, and samples were loaded on 12.5% SDS polyacrylamide gels and electrophoresis was performed. Proteins were detected with primary antibodies raised against occludin, tricellulin, or claudin-1, -2, -3, -4, -5, and -7, and β-actin. To detect bound antibodies, peroxidase-conjugated goat anti-rabbit IgG or goat anti-mouse IgG antibodies and the chemiluminescence detection system Lumi-LightPLUS Western blotting kit (Roche, Mannheim, Germany) were employed. Signals were detected employing a luminescence imager (Fusion FX7, Vilber Lourmat, France).

Chemicals

All chemicals, unless otherwise noted, were purchased from Sigma Aldrich.

Statistical Analysis

Data are expressed as mean ± standard error of the mean, with n indicating the number of experiments. Statistical analysis was performed using Student's *t*-test and Bonferroni-Holm adjustment for multiple comparisons. $P<0.05$ was considered significant with denotation as $*p<0.05$, $**p<0.01$, and $***p<0.001$.

RESULTS

Cell Viability After Incubation with Laurate

Cell viability was assessed by lactate dehydrogenase (LDH) release assay, indicating toxic conditions as cell injury causes

LDH release into the medium. The total LDH content of the cells after 30 min incubation with 2% Triton X-100 was set at 100% and LDH released into the medium was calculated accordingly. Whereas 2 h incubation with 3.5 mM laurate did not induce significant liberation of the enzyme, a concentration of 4.5 mM and 6 mM induced an increase in LDH release, as shown in Fig. 1 ($n=4$, respectively). Although these effects might have not been a mandatory reason for exclusion, further experiments were conducted at a concentration of 3.5 mM which also ensured a maximum solubility throughout all further experiments.

Transepithelial, Transcellular, and Paracellular Resistance

The application of 3.5 mM Na^+-laurate resulted in a substantial and reversible decrease in transepithelial resistance to 70.7±2.5% of initial TER after 30 min (***$p<0.001$, $n=12$, respectively), 63±3.8% after 60 min (***$p<0.001$), and 49.5±0.5% after 120 min (***$p<0.001$), whereas controls did not significantly change. After wash out, a complete reversibility to 93.6±8.4% was observed (Fig. 2a).

To discriminate between the resistance of the trans- and paracellular pathway, two-path impedance spectroscopy was employed as shown in Fig. 2b. In accordance with the previous data set, R^{epi} equalling TER was 415.9±35.6 Ω·cm^2 in controls, whereas after application of laurate, R^{epi} was 210.2±17.7 Ω·cm^2 (***$p<0.001$). While R^{trans} did not significantly change (685.7±67.8 Ω·cm^2 *vs.* 731.8±202.7 Ω·cm^2), R^{para} was markedly reduced after incubation with laurate (1,264±208.8 Ω·cm^2 *vs* 518.4±133.2 Ω·cm^2, *$p<0.05$), indicating an exclusively paracellular effect on barrier function ($n=7$, respectively).

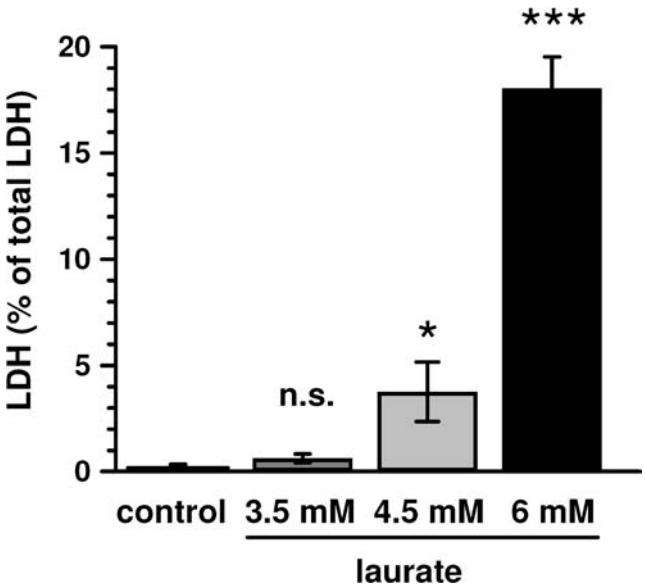

Fig. 1 Lactate dehydrogenase (LDH) cell viability assay. Cell viability under control conditions and after 2 h incubation with 3.5 mM, 4.5 mM and 6 mM laurate was tested. After 2 h incubation with 3.5 mM laurate, no significant change was observed (n.s.), whereas higher concentrations showed an increase of LDH release (*$p<0.05$, ***$p<0.001$, $n=4$, respectively).

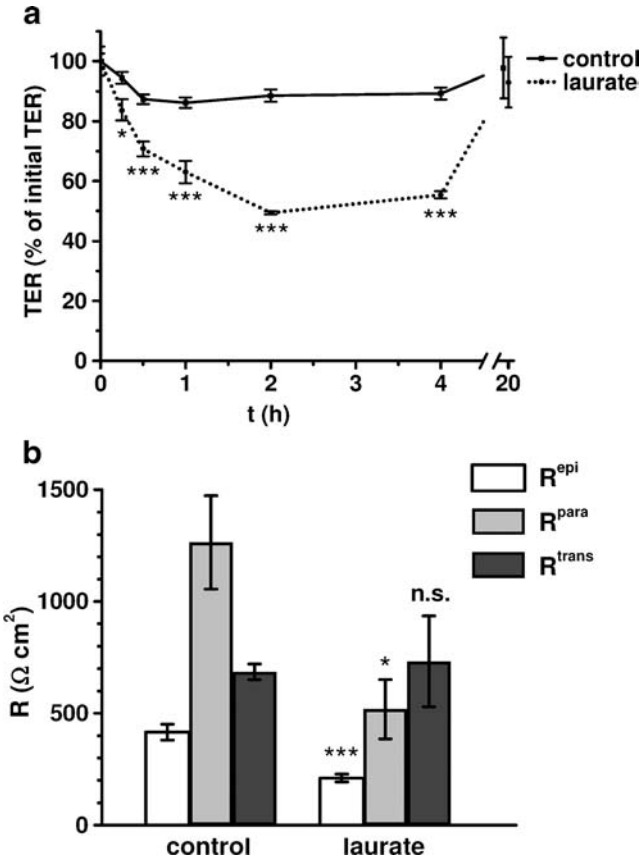

Fig. 2 Laurate effect on TER of HT-29/B6 monolayers. Incubation with 3.5 mM laurate induced a time-dependent decrease of transepithelial resistance (TER), which was reversible after wash out (; *$p<0.05$, ***$p<0.001$, $n=12$, respectively). (**b**) Two-path impedance spectroscopy. Laurate induced a decrease of the paracellular resistance R^{para}, whereas the transcellular resistance (R^{trans}) was not changed. Therefore, the effect on transepithelial resistance (R^{epi}) could be attributed to a pure effect on paracellular barrier properties (*$p<0.05$, ***$p<0.001$, $n=7$).

Paracellular Flux Markers

To evaluate the size selectivity of the paracellular pathway, the permeabilities for fluorescein (330 Da) and 4 kDa FITC-dextran were analyzed in unidirectional marker flux experiments as shown in Fig. 3. Laurate induced a strong increase of fluorescein permeability compared to controls (from 0.09±0.01 · 10^{-6} to 0.18±0.03 · 10^{-6} cm/s, **$p<0.01$, $n=8$ and 6, respectively, Fig. 3a). In contrast, permeability for 4 kDa FITC-dextran was not significantly changed (from 0.08±0.01 · 10^{-6} to 0.06±0.01 · 10^{-6} cm/s, $n=7$, respectively; Fig. 3b).

For further analysis of paracellular molecule permeation, monolayers were apically incubated with sulfo-NHS-SS-

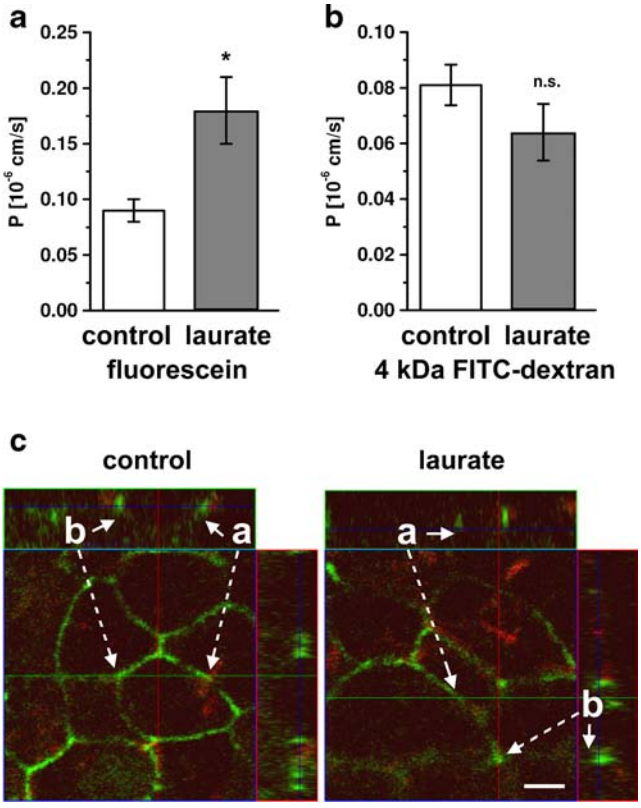

Fig. 3 Effect on paracellular marker permeability. (**a**) fluorescein, (**b**) 4 kDa FITC dextran, (**c**) sulfo-NHS-SS-biotin. Measurement of marker fluxes revealed an effect limited to the smaller fluorescein (330 Da), whereas 4 kDa FITC-dextran permeability was not affected. Moreover, no permeability for the membrane-impermeable marker molecule sulpho-NHS-SS-biotin (607 Da) within or below (**a**, *solid arrows*) bicellular or (**b**, *solid arrows*) tricellular TJ were observed by means of confocal laser scanning immunofluorescence microscopy allowing analysis of signals within lateral spaces by means of z-scans. The *dotted arrows* indicate the respective localization of bicellular and tricellular tight junctions in top views, bar: 5 μm.

biotin (607 Da, red) after treatment with laurate (Fig. 3c), and were then counter stained with anti-ZO-1 (green), a tight junction scaffolding protein co-localizing with the tight junction. Scanning of the lateral (z-) axis of the cells by means of confocal laser-scanning microscopy revealed no increase of permeation of the red biotin signals within or below (a) bicellular or (b) tricellular cell contacts, indicating a cut off for laurate-induced paracellular permeability for molecules between molecular masses of ~330 and 600 Da. As this method detects translocated biotin trapped in the intercellular space, the incomplete wash out of apical biotin indicated by the slight superficial red background signals, merely demonstrates the compound's detectability.

Analysis of the Cytoskeleton

To analyze laurate effects on the cytoskeleton, confocal laser-scanning immunofluorescence microscopy was employed analyzing F-actin staining of the cytoskeleton. Moreover, inhibitors

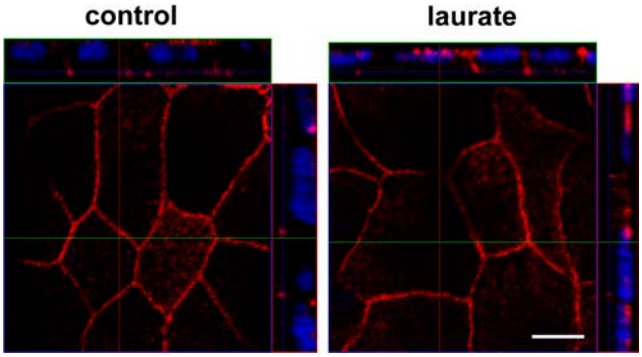

Fig. 4 Phalloidin-staining of the cytoskeleton. Immunostaining revealed no change in F-actin localization, indicating no detectable involvement of the cytoskeleton in laurate effects (bar: 5 μm).

of actin-myosin interaction were employed. Confocal images did not indicate changes of the cytoskeleton regarding the localization and integrity of F-actin (Fig. 4). Furthermore, pre-incubation with inhibitors of actin-myosin interaction as myosin

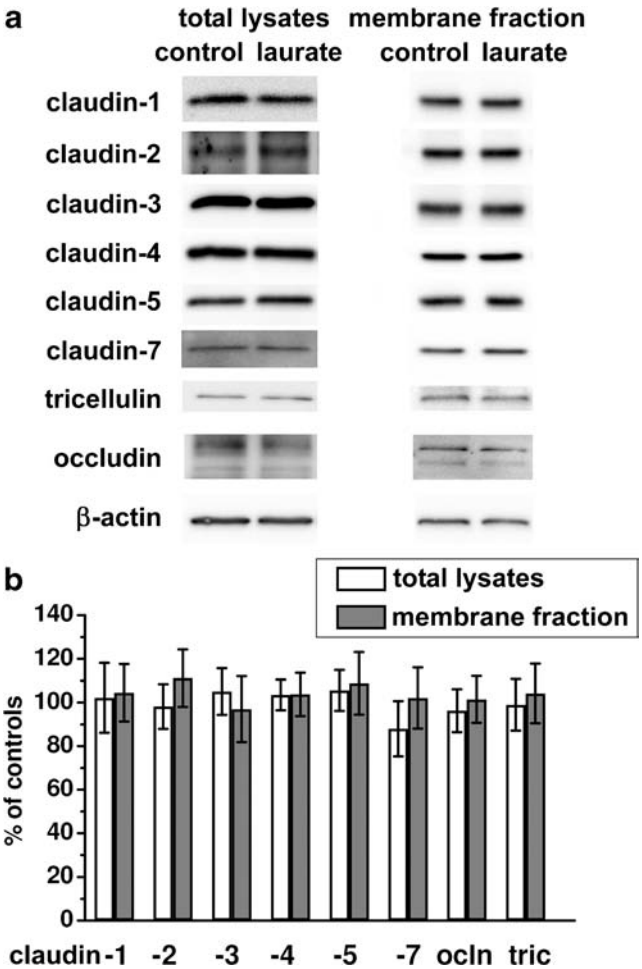

Fig. 5 Western blots. (**a**) Western blot analysis was performed analyzing laurate effects on tight junction proteins in total lysates and membrane fractions (120 min), showing strong and consistent signals for the tight junction proteins claudin-1, -2, -3, -4, -5 -7, and occludin, and tricellulin. (**b**) Densitometry. Considering endogenous β-actin signals as reference, no effects of laurate on TJ protein expressions were observed ($n = 6$, respectively).

light chain kinase blockers inhibitory peptide M18 (10^{-5} M, apical and basolateral) and Rho kinase inhibitor Y-27632 (10^{-5} M, apical and basolateral), did not inhibit the laurate effect on TER (63.6±6.42 and 67.97±11.7% of initial values), n.s. from laurate-only-controls, and effects of M18 and Y-27632 alone were not significantly different from controls without laurate (102.93±2.43 and 102.54±1.74% of initial values, $n=4$, respectively).

Abundance of Tight Junction Proteins

Western blots were performed including total lysates and crude membrane fractions of HT-29/B6 cells after 2 h incubation of confluent monolayers with 3.5 mM laurate. An isolated increase or decrease in crude membrane fraction proteins combined with persistently unaltered protein signals in total lysates would have suggested a removal or introduction of proteins from or into the cell membrane possibly due to laurate effects. However, detection of tight junction proteins claudin-1, -2, -3, -4, -5, and -7, occludin, and tricellulin revealed strong and consistent signals in both preparations, with no obvious changes between controls and protein preparations of monolayers incubated with laurate (Fig. 5a).

Densitometry revealed no significant changes after incubation with laurate compared to respective control signals of total lysates and membrane fractions ($n=6$, respectively, Fig. 5b). Taking into account the respective β-actin signals of selfsame preparations, claudin signals were 102.2±16.0% and 104.5±13.2% (claudin-1), 98.2±10.3% and 111.1±13.2% (claudin-2),105.0±10.7% and 96.9±15.1% (claudin-3), 103.5±7.0% and 103.7±9.9% (claudin-4), 105.5±9.3% and 108.8±14.3% (claudin-5), and 88.0±12.7% and 102.1±14.1% (claudin-7) of respective control signals set to 100%. Moreover, measurement of TAMP signals revealed 96.3±9.9% and 101.4±10.7% (occludin), and 99.0±11.8% and 104.2±13.6% (tricellulin) of respective control signals set to 100%, suggesting no change in abundance of major barrier-determining tight junction proteins during incubation with laurate leading to the substantial decrease of transepithelial resistance and selective opening of the paracellular pathway for fluorescein.

Localization of Tight Junction Proteins

Tight junction proteins contribute to barrier or channel functions only if properly localized within the tight junction. In most cases, membrane protein abundance and immunofluorescence localization of claudins are in accordance. However, these results can diverge, indicating that a tight junction protein exists within the cell membrane, but localized apart from the tight junction (24). Occludin, claudin-1, -3, and tricellulin localizations were not altered after laurate treatment in immunofluorescent stainings (Fig. 6). In contrast, however, one major gastrointestinal barrier-forming tight junction protein, claudin-5, showed reduced localization within the tight junction after incubation with laurate. This effect was reversible after wash-out (Fig. 7). This suggests a mechanism by which laurate causes claudin-5 to be removed from the tight junction, thus transiently opening the epithelial seal for the passage of solutes.

DISCUSSION

The aim of this study was to analyze the effects of laurate on transepithelial resistance, paracellular permeability and the distribution of tight junction proteins in confluent monolayers

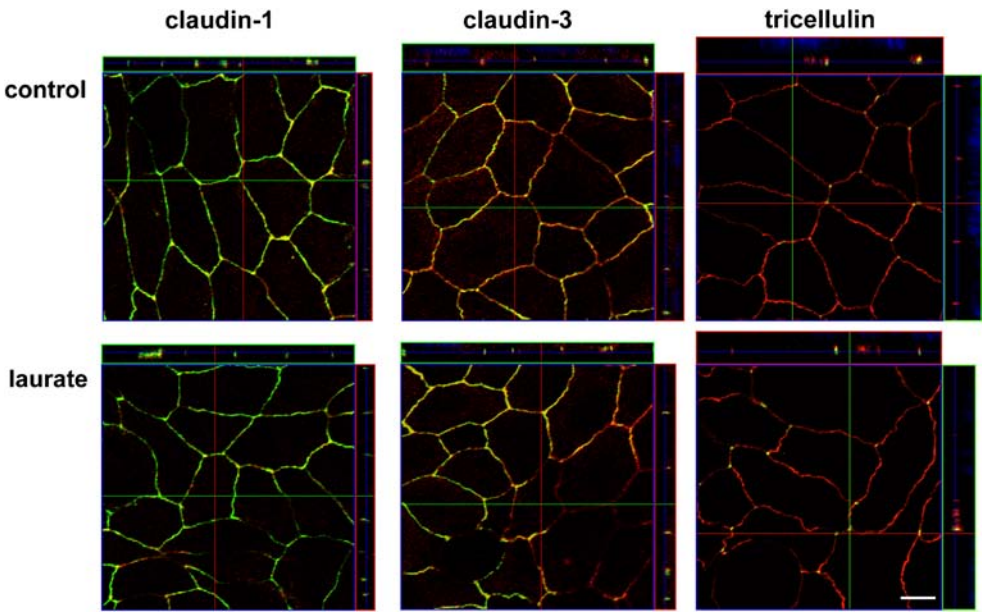

Fig. 6 Detection of occludin, claudin-1, -3, and tricellulin by confocal laser-scanning immunofluorescence microscopy. Immunostainings revealed no change of localization of claudin-1 and claudin-3 (*red*, counter-staining of occludin in *green*, respectively), and tricellulin (*green*, for best visibility counter-staining of occludin in *red*; bar: 5 μm).

of the intestinal epithelial cell line HT-29/B6. Both the epithelium's endogenous expression of various tight junction proteins of the TAMP and claudin families (14,25) as well as the close correspondence of observations in HT-29/B6 with those found in rodent and human epithelia (26,27) commend HT-29/B6 as a suitable model for the analysis of colonic barrier properties (23). Experimental concentrations of laurate were chosen in respect to the imperative of permeability enhancer non-toxicity. A range of concentrations for which no harmfulness had been suggested (15) was then tested using LDH as a parameter for cell injury. 3.5 mM laurate was the highest possible yet physiological concentration that did not significantly increase the cell's LDH release.

Exposure with 3.5 mM laurate resulted in a substantial and reversible decrease in transepithelial resistance down to 50% of initial values. This was identified to be the result of an exclusive drop in paracellular resistance R^{para} by two-path impedance spectroscopy, while transcellular resistance R^{trans} remained constant throughout experiments. Full reversibility of the effect occurred, yet with some delay at approximately 18 h after wash-out, requiring further and comparative research both *in vitro* and *in vivo* in order to assess the consequences of prolonged paracellular permeation.

In accordance with the changes in resistance indicative of a specifically paracellular effect, exposure with 3.5 mM laurate induced a marked increase in the permeability for fluorescein (330 Da). However, permeability for sulpho-NHS-SS-biotin (607 Da) and FITC-dextran (4 kDa) did not increase.

Confocal laser-scanning microscopy revealed a decrease of claudin-5 within tight junction complexes for laurate, without effects on either expression or distribution of other tight junction proteins such as tricellulin, a barrier former preventing the paracellular passage of macromolecules.

This contrasts recent findings in HT-29/B6 cells for caprate (C10), another medium-chain fatty acid, that affected not only claudin-5 but tricellulin, thereby opening the paracellular passage for a much larger range of solutes up to 10 kDa (14).

The functions of both claudin-5 and tricellulin, targets discussed in the context of caprate and laurate effects, have previously been characterized by our group. Tricellulin emerged as a major determinant preventing the paracellular passage of macromolecules (28), while claudin-5 contributes to the barrier against the paracellular passage of ions and small molecules such as [^{3}H]-mannitol (25). The exact regulatory mechanisms involved in retrieval of claudin-5 still remain to be elucidated, but a number of experiments have excluded an involvement of the cytoskeleton and a variety of kinases. However, the high velocity of the effects might indicate a direct interaction with membrane microdomains carrying claudin-5.

While the mechanisms of both claudin-5 and tricellulin reduction within the tight junction appear to have been linked in the case of caprate, laurate showed an isolated effect on claudin-5, thereby dismissing a mandatory link between the two. Cause for these differing mechanisms may be found in the different chemical natures of the compounds, with the smaller-sized caprate (C10) possibly displaying a more efficient access to the target site in tricellular tight junctions. However, more in-depth analyses of tight junction protein interaction and dynamic regulation of the tight junction within epithelia require further investigation, as detailed information on the molecular assembly of claudins within the tight junction is scarce (29). Earlier results for claudin-5 indicate that protein assembly takes place in the paracellular space with polymerization of claudin-5 via trans-interaction of molecules of the opposing lateral cell membranes (30).

Having initially been identified in endothelia and primarily attributed to barrier function of the blood–brain-barrier

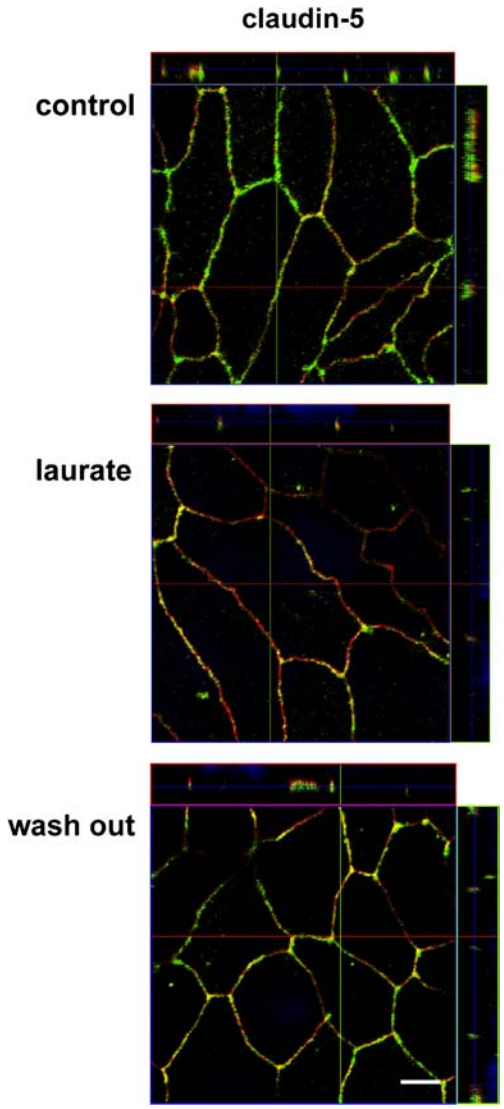

Fig. 7 Detection of occludin and claudin-5 by confocal laser-scanning immunofluorescence microscopy. Laurate induced a decrease of claudin-5 signals (*green*, counter-staining of occludin in *red*), which was reversible after wash-out (bar: 5 μm).

(31,32), claudin-5 has been found to be a determinant for the sealing properties of the tight junction in gastrointestinal epithelium (6,33). Moreover, claudin-5 has been detected in tight junctions of pancreatic acinar cells (34), Schwann cells (35), and alveolar epithelial cells (36). Moreover, claudin-5 plays a crucial role during ontogenesis (37,38).

A recent functional characterization within the scope of cloning claudin-5 cDNA from the human intestinal cell line HT-29/B6 and inducing overexpression in Caco-2 cells by stable transfection demonstrated its contribution to epithelial barrier properties in more detail. Compared to vector-transfected control cells, claudin-5-transfected cells displayed a strong increase in TER and a marked decrease in permeability for the paracellular flux marker [^{3}H]-mannitol (182 Da) (25). These findings are in accordance with functional effects observed after retrieval of claudin-5 from the tight junction, as in our present study with laurate inducing (i) a drop of TER to 50% of initial values, and (ii) an increased permeability of the flux marker fluorescein (330 Da) without significant effects on the permeability for sulfo-NHS-SS-biotin (607 Da) or 4 kDa FITC dextran.

Laurate esters are a natural component of a variety of foods including cow's and human milk with concentrations of up to 6.4% of total fat (19,20). High concentrations of laurate might also contribute to absorptive functions in the infant's intestine, though free lauric acid concentration in milk has been shown to be rather limited (39). However, additional factors such as whey enhancing, and caprate decreasing barrier properties have been analyzed in the selfsame model, namely HT-29/B6 cells (14,40). Furthermore, accumulation of milk has been demonstrated to have an additional effect on tight junctions in mammary glands (41). Regarding the effects of milk on paracellular transport and barrier function of the intestinal epithelium, however, the interaction of absorption-enhancing factors such as caprate and laurate, and barrier-strengthening factors, such as whey, requires further research.

Claudin-5 has been described as a potential target in the development of novel drug targeting and drug delivery strategies, after it had been demonstrated that the tight junction protein turned out to be affected by caprate (14,42). As claudin-5 is expressed in intestinal epithelia as well as in the endothelium, it is not only discussed as a target for induction of bioavailability after gastrointestinal uptake, but also in context with its role in the blood brain barrier. However, relevant effective blood concentrations of laurate after oral intake cannot be expected, as the natural occurence of laurate in food also indicates proper and effective metabolism of laurate within the body.

While caprate (C10) is employed as a component of a rectal suppository as well as in a permeability-enhancing formulation already in clinical trial (5,16), applications for laurate, which has also been suggested for absorption enhancement, still remain to be elucidated (15).

Potential applications may include a combination with ampicillin (349 Da), as it is of similar size to the 330 Da fluorescein and may benefit from the permeating effects of laurate. While the Ringer's solution used in our experiments had a sufficient buffer capacity to avoid effects of solutes on pH, and employed flux markers were not charged, solute charge might also affect permeability, and should be considered specifically in further approaches regarding the refinement of pharmaceutical applications. However, the adverse effects of an unwanted passage of larger-scale immunomodulatory or toxic agents may be minimized in laurate when compared to caprate.

CONCLUSIONS

Laurate induces a specific opening of the paracellular pathway in the human intestinal epithelial model system HT-29/B6. This effect is based on a reversible relocation of claudin-5, a tightening tight junction protein limiting the paracellular passage for ions and molecules up to 330 Da, whereas permeability for the larger marker molecules sulpho-NHS-SS-biotin (607 Da) and 4 kDa FITC dextran appeared unaffected. Therefore, laurate is a promising candidate for epithelial drug delivery strategies for small drug molecules of approximately the size of fluorescein. In contrast to the effect of the absorption enhancer caprate which simultaneously affects both claudin-5 and tricellulin, the laurate effect is limited to claudin-5, with separate pathways for the relocation of tricellulin and claudin-5 pointing towards independent rapid and reversible mechanisms of tight junction protein regulation and distribution within tight junction complexes.

ACKNOWLEDGMENTS AND DISCLOSURES

We thank Detlef Sorgenfrei, In-Fah M. Lee, and Anja Fromm for their expert technical assistance. This work was supported by grants of the Deutsche Forschungsgemeinschaft (Grants DFG FOR 721/2, DFG SFB 852), and the St. Petersburg State University (Grant SPbGU 1.37.118.201).

REFERENCES

1. Döring F, Walter J, Will J, Föcking M, Boll M, Amasheh S, *et al.* Delta-aminolevulinic acid transport by intestinal and renal peptide transporters and its physiological and clinical implications. J Clin Invest. 1998;101(12):2761–7.
2. Döring F, Will J, Amasheh S, Clauss W, Ahlbrecht H, Daniel H. Minimal molecular determinants of substrates for recognition by the intestinal peptide transporter. J Biol Chem. 1998;273(36):23211–8.
3. Guo A, Hu P, Balimane PV, Leibach FH, Sinko PJ. Interactions of a non-peptidic drug, valacyclovir, with the human intestinal peptide

transporter (hPEPT1) expressed in a mammalian cell line. J Pharmacol Exp Ther. 1999;289(1):448–54.
4. Rosenthal R, Heydt MS, Amasheh M, Stein C, Fromm M, Amasheh S. Analysis of absorption enhancers in epithelial cell models. Ann N Y Acad Sci. 2012;1258:86–92.
5. Aungst BJ. Absorption enhancers: applications and advances. AAPS J. 2012;14(1):10–8.
6. Markov AG, Veshnyakova A, Fromm M, Amasheh M, Amasheh S. Segmental expression of claudin proteins correlates with tight junction barrier properties in rat intestine. J Comp Physiol B. 2010; 180(4):591–8.
7. Furuse M, Hata M, Furuse K, Yoshida Y, Haratake A, Sugitani Y, *et al.* Claudin-based tight junctions are crucial for the mammalian epidermal barrier: a lesson from claudin-1-deficient mice. J Cell Biol. 2002;156(6):1099–111.
8. Günzel D, Yu AS. Claudins and the modulation of tight junction permeability. Physiol Rev. 2013;93(2):525–69.
9. Furuse M, Fujita K, Hiiragi T, Fujimoto K, Tsukita S. Claudin-1 and -2: novel integral membrane proteins localizing at tight junctions with no sequence similarity to occludin. J Cell Biol. 1998;141(7):1539–50.
10. Furuse M, Hirase T, Itoh M, Nagafuchi A, Yonemura S, Tsukita S, *et al.* Occludin: a novel integral membrane protein localizing at tight junctions. J Cell Biol. 1993;23(6):1777–88.
11. Ikenouchi J, Furuse M, Furuse K, Sasaki H, Tsukita S, Tsukita S. Tricellulin constitutes a novel barrier at tricellular contacts of epithelial cells. J Cell Biol. 2005;171(6):939–45.
12. Raleigh DR, Marchiando AM, Zhang Y, Shen L, Sasaki H, Wang Y, *et al.* Tight junction-associated MARVEL proteins marveld3 tricellulin and occludin have distinct but overlapping functions. Mol Biol Cell. 2010;21(7):1200–13.
13. Rosenthal R, Günzel D, Finger C, Krug SM, Richter JF, Schulzke JD, *et al.* The effect of chitosan on transcellular and paracellular mechanisms in the intestinal epithelial barrier. Biomaterials. 2012;33(9):2791–800.
14. Krug SM, Amasheh M, Dittmann I, Christoffel I, Fromm M, Amasheh S. Sodium caprate as an enhancer of macromolecule permeation across tricellular tight junctions of intestinal cells. Biomaterials. 2013;34(1):275–82.
15. Lindmark T, Kimura Y, Artursson P. Absorption enhancement through intracellular regulation of tight junction permeability by medium chain fatty acids in Caco-2 cells. J Pharmacol Exp Ther. 1998;284(1):362–9.
16. Lindmark T, Söderholm JD, Olaison G, Alván G, Ocklind G, Artursson P. Mechanism of absorption enhancement in humans after rectal administration of ampicillin in suppositories containing sodium caprate. Pharm Res. 1997;14(7):930–5.
17. Lindmark T, Nikkilä T, Artursson P. Mechanisms of absorption enhancement by medium chain fatty acids in intestinal epithelial Caco-2 cell monolayers. J Pharmacol Exp Ther. 1995;275(2):958–64.
18. Maher S, Leonard TW, Jacobsen J, Brayden DJ. Safety and efficacy of sodium caprate in promoting oral drug absorption: from in vitro to the clinic. Adv Drug Deliv Rev. 2009;61(15):1427–49.
19. Francois CA, Connor SL, Wander RC, Connor WE. Acute effects of dietary fatty acids on the fatty acids of human milk. Am J Clin Nutr. 1998;67(2):301–8.
20. Moltó-Puigmartí C, Castellote AI, Carbonell-Estrany X, López-Sabater MC. Differences in fat content and fatty acid proportions among colostrum, transitional, and mature milk from women delivering very preterm, preterm, and term infants. Clin Nutr. 2011;30(1):116–23.
21. Zenger V, Laurate C. US Food and Drug Administration. High laurate canola oil. BNF No.25. 1995. http://www.fda.gov/Food/FoodScienceResearch/Biotechnology/Submissions/ucm161141.htm. Accessed 28 February 2014.
22. Kreusel KM, Fromm M, Schulzke JD, Hegel U. Cl^- secretion in epithelial monolayers of mucus-forming human colon cells (HT-29/B6). Am J Physiol. 1991;261(4):C574–82.
23. Krug SM, Fromm M, Günzel D. Two-path impedance spectroscopy for measuring paracellular and transcellular epithelial resistance. Biophys J. 2009;97(8):2202–11.
24. Amasheh S, Meiri N, Gitter AH, Schöneberg T, Mankertz J, Schulzke JD, *et al.* Claudin-2 expression induces cation-selective channels in tight junctions of epithelial cells. J Cell Sci. 2002; 115(24):4969–76.
25. Amasheh S, Schmidt T, Mahn M, Florian P, Mankertz J, Tavalali S, *et al.* Contribution of claudin-5 to barrier properties in tight junctions of epithelial cells. Cell Tissue Res. 2005;321(1): 89–96.
26. Amasheh M, Luettig J, Amasheh S, Zeitz M, Fromm M, Schulzke JD. Effects of quercetin on the colonic cell culture model HT-29/B6 and rat intestine in vitro. Ann N Y Acad Sci. 2012;1258:100–7.
27. Amasheh S, Milatz S, Krug SM, Bergs M, Amasheh M, Schulzke JD, *et al.* Na^+ absorption defends from paracellular back-leakage by claudin-8 upregulation. Biochem Biophys Res Commun. 2009;378(1):45–50.
28. Krug SM, Amasheh S, Richter JF, Milatz S, Günzel D, Westphal JK, *et al.* Tricellulin forms a barrier to macromolecules in tricellular tight junctions without affecting ion permeability. Mol Biol Cell. 2009; 20(16):3713–24.
29. Anderson JM, Van Itallie CM. Physiology and function of the tight junction. Cold Spring Harb Perspect Biol. 2009;1(2): a002584.
30. Piontek J, Winkler L, Wolburg H, Müller SL, Zuleger N, Piehl C, *et al.* Formation of tight junction: determinants of homophilic interaction between classic claudins. FASEB J. 2008;22:146–58.
31. Morita K, Sasaki H, Furuse M, Tsukita S. Endothelial claudin: claudin-5/TMVCF constitutes tight junction strands in endothelial cells. J Cell Biol. 1999;147(1):185–94.
32. Nitta T, Hata M, Gotoh S, Seo Y, Sasaki H, Hashimoto N, *et al.* Size-selective loosening of the blood-brain barrier in claudin-5-deficient mice. J Cell Biol. 2003;161(3):653–60.
33. Amasheh S, Fromm M, Günzel D. Claudins of intestine and nephron - a correlation of molecular tight junction structure and barrier function. Acta Physiol. 2011;201(1):133–40.
34. Rahner C, Mitic LL, Anderson JM. Heterogeneity in expression and subcellular localization of claudins 2, 3, 4, and 5 in the rat liver, pancreas, and gut. Gastroenterology. 2001;120(2):411–22.
35. Poliak S, Matlis S, Ullmer C, Scherer SS, Peles E. Distinct claudins and associated PDZ proteins form different autotypic tight junctions in myelinating Schwann cells. J Cell Biol. 2002;159(2): 361–72.
36. Wang F, Daugherty B, Keise LL, Wei Z, Foley JP, Savani RC, *et al.* Heterogeneity of claudin expression by alveolar epithelial cells. Am J Respir Cell Mol Biol. 2003;29(1):62–70.
37. Sirotkin H, Morrow B, Saint-Jore B, Puech A, Das Gupta R, Patanjali SR, *et al.* Identification, characterization, and precise mapping of a human gene encoding a novel membrane-spanning protein from the 22q11 region deleted in velo-cardio-facial syndrome. Genomics. 1997;42(2):245–51.
38. Kojima S, Rahner C, Peng S, Rizzolo LJ. Claudin 5 is transiently expressed during the development of the retinal pigment epithelium. J Membr Biol. 2002;186(2):81–8.
39. Amer B, Nebel C, Bertram HC, Mortensen G, Hermansen K, Dalsgaard TK. Novel method for quantification of individual free fatty acids in milk using an in-solution derivatisation approach and gas chromatography-mass spectrometry. Int Dairy J. 2013;32:199–203.
40. Hering NA, Andres S, Fromm A, van Tol EA, Amasheh M, Mankertz J, *et al.* Transforming growth factor-β, a whey protein component, strengthens the intestinal barrier by up-regulating claudin-4 in HT-29/B6 cells. J Nutr. 2011;141(5): 783–9.

41. Markov AG, Kruglova NM, Fomina YA, Fromm M, Amasheh S. Altered expression of tight junction proteins in mammary epithelium after discontinued suckling in mice. Pflugers Arch. 2012;463(2): 391–8.

42. Del Vecchio G, Tscheik C, Tenz K, Helms HC, Winkler L, Blasig R, *et al.* Sodium caprate transiently opens claudin-5-containing barriers at tight junctions of epithelial and endothelial cells. Mol Pharm. 2012;9(9):2523–33.